

# Dynamics of localized and nonlocalized optical vortex solitons in cubic-quintic nonlinear media

V. I. Berezhiani

*Graduate School of Frontier Sciences, The University of Tokyo, Hongo 7-3-1, Tokyo 113-0033, Japan*

V. Skarka

*Laboratoire POMA, UMR 6136 CNRS, Université d'Angers, 2, Boulevard Lavoisier, 49045 Angers, cedex 1, France*

N. B. Aleksić

*Institute of Physics, Pregrevica 118, 11000 Belgrade, Yugoslavia*

(Received 25 January 2001; revised manuscript received 1 June 2001; published 18 October 2001)

The nonlinear dynamics of laser beams carrying phase singularity in media with cubic-quintic nonlinearity changing from self-focusing to self-defocusing is examined. A novel kind of stable nonlocalized optical vortices appears in such media as well as localized vortex solitons. Linear stability analysis and numerical simulations show the stability of localized vortices only in the defocusing region.

DOI: 10.1103/PhysRevE.64.057601

PACS number(s): 42.65.Tg

The generation, propagation, and interaction of optical vortices in nonlinear media have been the subject of extensive studies. In a self-defocusing media transverse instability of dark solitary stripe results in the generation of an optical vortex soliton (OVS). These solitons are  $(2+1)$ -dimensional (two “transverse” and a propagation dimension) stationary beam structures with phase singularity and nonzero angular momentum. An OVS is a dark spot, i.e., a zero intensity center surrounded by a bright infinite background. Generation, dynamics, and interactions of an OVS exhibit interesting features and are the subject of ongoing theoretical and experimental research [1]. Self-focusing media also support localized soliton solutions with phase dislocation surrounded by one or many bright rings. To distinguish these solitonic structures from OVS's which have nonzero asymptotes at infinity we term them as localized optical vortex solitons (LOVS). Recently, it was shown that LOVS are unstable against symmetry breaking perturbations that lead to the breakup of rings into filaments [2]. These filaments form the stable bright solitons which, like free Newtonian particles, fly off tangentially to the initial rings conserving total angular momentum [3].

Either OVS or LOVS can be generated using an input light beam with an externally superimposed vortex structure. Such beams are known in optics as “singular beams” and can be readily generated using different techniques, for instance, computer synthesized holograms and prescribed phase masks [4]. At the singularity the field amplitude is strictly zero while the phase becomes undetermined. Angular momentum of the beam is proportional to  $mN$ , where  $N$  is the beam power and integer  $m$  defines its topological charge.

In this paper we study the dynamics of a self-trapped singular beam in saturating nonlinear media. We investigate the generation and dynamics of OVS and LOVS. As a model nonlinearity we consider the cubic-quintic saturating nonlinearity. This kind of nonlinearity has been widely applied in different domains of research not only in nonlinear optics but also in plasma physics [5] as well as in the context of Bose superfluid [6]. Taking into account that some of the materials currently used in optical systems exhibit weak saturation ef-

fects, their nonlinearity can be approximated with good accuracy by the cubic-quintic model.

Recent measurements show that the polydiacetylene *para*-toluene sulfonate (PTS) exhibits this kind of saturating nonlinearities with large cubic-quintic indices [7]. Moreover, the nonlinear index of refraction becomes negative at the peak while remaining positive in the wings of the beam intensity profile. Being a self-focusing medium, PTS can exhibit at higher intensity features of defocusing media. We show that due to this peculiarity in such a material it is possible to create both LOVS and OVS.

The dynamics of vortices in nonlinear materials is based on the analysis of a  $(2+1)$ -dimensional nonlinear Schrödinger equation (NSE)

$$2ik \frac{\partial \mathcal{E}}{\partial z} + \Delta_{\perp} \mathcal{E} + 2k^2 \frac{\delta n(|\mathcal{E}|^2)}{n_0} \mathcal{E} = 0, \quad (1)$$

where  $\mathcal{E}$  is a slowly varying field envelope,  $n_0$  and  $\delta n(|\mathcal{E}|^2)$  are, respectively, linear and nonlinear optical indices,  $\Delta_{\perp} = \partial^2/\partial x^2 + \partial^2/\partial y^2$  is the two-dimensional Laplacian describing beam diffraction, and  $k$  is a wave vector. In order to prevent the wave collapse the saturating nonlinearity is required. The nonlinear index of refraction (NIR) corresponding to PTS is established to be  $\delta n = n_2 I + n_4 I^2$ , where  $I = n_0 c |\mathcal{E}|^2 / 4\pi$  is the intensity of the electromagnetic (EM) radiation. For the  $\lambda = 1.6 \mu\text{m}$  laser radiation the measured values of second- and fourth-order optical indices are, respectively,  $n_2 = 2.2 \times 10^{-3} \text{ cm}^2/\text{GW}$  and  $n_4 = -0.8 \times 10^{-3} \text{ cm}^4/\text{GW}^2$ . The critical intensity at the peak of the pulse profile giving  $\delta n = 0$  is  $I_0 = |n_2/n_4| = 2.75 \text{ GW}/\text{cm}^2$ . Such a self-focusing medium ( $d\delta n/dI > 0$ ) at higher intensity,  $I > 0.5I_0$ , becomes defocusing, i.e., NIR changes have a negative slope. For the peak intensity  $I_m > 0.5I_0$  the NIR becomes defocusing at the peak while remaining focusing at the wings of the laser beam intensity profile. A spatial ring formation has been observed in PTS due to the nonlinearity sign changes at the beam center when the beam intensity  $I_m (\approx 8 \text{ GW}/\text{cm}^2)$  is above the critical one [7].

Equation (1) can be rewritten in dimensionless form as

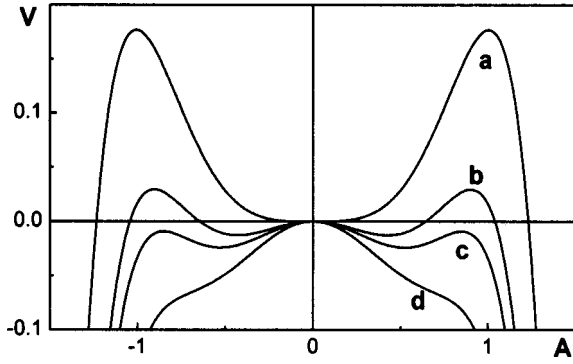


FIG. 1. Potential as a function of the amplitude for different values of the propagation constant  $\beta$ .

$$i \frac{\partial E}{\partial z} + \Delta_{\perp} E + f(|E|^2)E = 0, \quad (2)$$

where the nonlinear function  $f(|E|^2)$  is

$$f(|E|^2) = |E|^2 - |E|^4. \quad (3)$$

The following normalizations are used:  $z/Z$ ,  $r_{\perp}/R$ , and  $I/I_0$  where  $Z = \lambda/(2\pi n_2 I_0)$  and  $R = \lambda/(8\pi^2 n_0 n_2 I_0)$ .

Let us now consider the soliton solutions carrying vortices. Assuming that solutions in polar coordinates are of the form  $E = A(r)\exp(im\theta + i\beta z)$ , Eq. (2) reduces to an ordinary differential equation

$$\frac{d^2 A}{dr^2} + \frac{1}{r} \frac{dA}{dr} - \beta A - \frac{m^2}{r^2} A + A^3 - A^5 = 0, \quad (4)$$

where  $A$  is  $r$ -dependent amplitude,  $\beta$  is a propagation constant, and  $m (\neq 0)$  is an integer known as the topological charge of optical vortex.

Numerically obtained solutions of Eq. (4) with both boundaries at zero correspond to the LOVS, while the OVS has a nonzero constant field background  $A_{\infty}$ . Asymptotic formulas for LOVS are  $A(r \rightarrow 0) \rightarrow r^{|m|} c_1$  and  $A(r \rightarrow \infty) \rightarrow c_1 r^{-1/2} \exp(-r\sqrt{\beta})$ . OVS solutions have the same asymptote for  $r \rightarrow 0$  while for  $r \rightarrow \infty$  the amplitude has a nonzero value  $A(r) = A_{\infty} + m^2/(r^2 f'(A_{\infty}))$ . Here,  $\beta = f(A_{\infty})$  and  $f'(A_{\infty}) < 0$  provided  $A_{\infty}^2 > 0.5$ . In dimensional units this condition corresponds to the negative slope of NIR ( $d\delta n/dI < 0$ ), i.e., in the asymptotic region of the solution [ $I(r) > 0.5I_0$ ] the medium is defocusing.

In order to obtain a better understanding we use the analogy with a nonconservative motion of a particle. Indeed, Eq. (4) can be rewritten as

$$\frac{d}{dr} \left[ \left( \frac{dA}{dr} \right)^2 + V(A) \right] = \frac{m^2}{r^2} \frac{dA^2}{dr} - \frac{2}{r} \left( \frac{dA}{dr} \right)^2, \quad (5)$$

where the ‘‘effective potential’’ is  $V(A) = -\beta A^2 + A^4/2 - A^6/3$ .

The profile of the potential  $V(A)$  for different values of the propagation constant  $\beta$  is presented in Fig. 1. If  $\beta \leq 0$ , the potential has a minimum at the point  $A=0$  and maxima

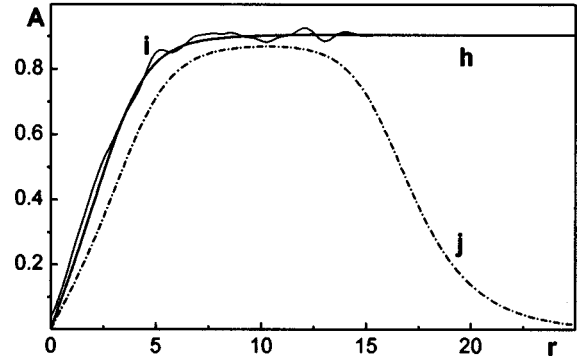


FIG. 2. Stationary OVS solution for  $\beta=0.16$  ( $h$ ). Damping of the perturbed OVS solution ( $i$ ). Stationary LOVS solution for  $\beta=0.18$  ( $j$ ).

at points  $A_{\max} = \pm[0.5 + (0.25 + |\beta|)^{1/2}]^{1/2}$  (see curve  $a$  in Fig. 1). For  $\beta > 0$  the potential acquires minima at points  $A_{\min} = \pm[0.5 - (0.25 - \beta)^{1/2}]^{1/2}$  (curve  $b$  in Fig. 1). If  $\beta > 3/16$  the potential maxima become negative (curve  $c$ ). For  $\beta > 1/4$  the lateral maxima vanish (see line  $d$ ).

The numerically obtained LOVS solutions of Eq. (4) correspond to the ‘‘effective particle’’ beginning its motion at origin and returning back asymptotically to the initial position. Such solutions exist for  $0 < \beta \leq 3/16$  where the potential has a shape similar to curve  $b$  in Fig. 1. The maximum amplitude of LOVS is bounded from above by the condition  $A_m < |A_{\max}(3/4)| \approx 0.87$ . For  $m=1$  and for given  $\beta$  the ‘‘particle’’ with ‘‘initial velocity’’  $A'(0) = c_1$ , in its way back due to the ‘‘damping,’’ cannot overpass the potential maximum at  $(0,0)$ -point. However, increasing its initial velocity the particle can make many oscillations between both potential wells before its final asymptotic settlement at origin; such solutions of Eq. (4) correspond to many rings LOVS. For the critical velocity, the effective particle reaches asymptotically the higher maximum of the potential; this solution corresponds to the OVS (line  $h$  in Fig. 2). With increase of  $\beta$  the central part of the LOVS flattens [8] and widens converging to the OVS (line  $j$  in Fig. 2). In principle, it is possible to create LOVS with a large transverse width. Notice that the bulk part of such flattened LOVS is in the region of defocusing NIR. The NSE admits both LOVS and OVS solutions. Their coexistence is mainly possible due to the particular cubic-quintic nonlinearity changing from the self-focusing to the self-defocusing one. The switching from LOVS to OVS and vice versa may be used in information processing.

In other domains of the parameter  $\beta$  LOVS solutions do not exist while OVS still appears. Indeed, OVS solutions are generated for  $\beta \leq 0$  corresponding to the potential shape similar to curve  $a$  (in Fig. 1). We also found out that the OVS solutions exist for  $\beta > 3/16$  (see curve  $c$ ). In other words, the ‘‘effective particle’’ cannot overpass but only approach asymptotically the lower potential maximum. For further increases of  $\beta$  lateral maximum is not high enough to stop the particle. For  $\beta > 1/4$  solutions are no more bounded (see curve  $d$ ). Numerical simulations for a single charge show that the stable OVS appears for  $\beta < 3/16$  ( $A_{\infty}^2 > 0.75$ ).

It is usually believed that for the ordinary self-defocusing

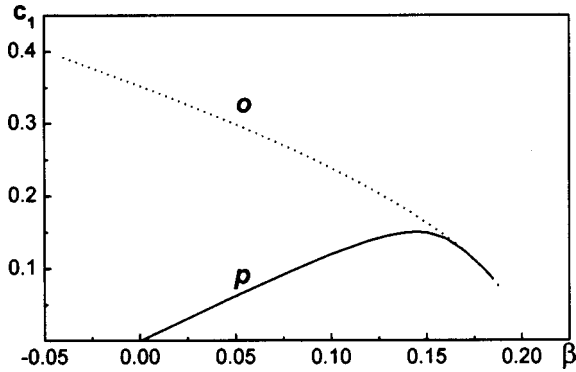


FIG. 3. Field derivative at the origin versus propagation constant  $\beta$  for OVS ( $o$ ) and LOVS ( $p$ ).

media “single-charged” OVS are topologically stable whereas vortices with a larger value of  $m$  may decay into the single-charged one [1]. We would like to emphasize that in the case of cubic-quintic nonlinearity the same beam can contain regions with not only defocusing but also focusing NIR. Indeed, near its center ( $r=0$ ) such a novel kind of OVS is in the focusing regime. Already for small radius  $r$  amplitude maximum (larger than 0.707) is reached corresponding to the defocusing NIR.

The intensity dependent switching from the focusing to defocusing regime influences the stability properties. Some insight can be obtained comparing the behavior of the field derivative at the origin  $c_1$  as a function of the propagation parameter  $\beta$  for a single charged OVS (dotted line  $o$  in Fig. 3) and LOVS (full line  $p$  similar to the one in Ref. [8]). The bulk of the OVS is always in the defocusing regime. Thus on the monotonically decreasing curve deepening of the potential near the origin (see Fig. 1) for larger  $\beta$  will be balanced by a decrease of the “initial velocity”  $c_1$ . The LOVS has the same behavior on the negative slope of the curve  $p$ , i.e., for  $\beta$  larger than the maximum ( $\beta=0.145$ ) in the self-defocusing region. However, on the positive slope of  $p$  ( $\beta < 0.145$ ), in the self-focusing region, the effects due to the increase of  $\beta$  are enhanced by the increase of the “initial velocities”  $c_1$ .

In order to perform linear stability analysis of both OVS and LOVS the assumed steady state solution is perturbed

$$E = \{A(r) + [a^+(r, z) \exp(iL\theta) + a^-(r, z) \times \exp(-iL\theta)]\} \exp(im\theta + i\beta z), \quad (6)$$

where  $a^\pm \ll A$  and azimuthal index  $L = 1, 2, 3, \dots$

Substituting such a solution in Eq. (2) and linearizing with respect to the perturbations the following coupled equations are obtained:

$$Q^\pm a^\pm + A^2(1 - 2A^2)(a^\mp)^* = 0, \quad (7)$$

where operator  $Q^\pm$  reads

$$Q^\pm = i \frac{\partial}{\partial z} - \beta + \frac{1}{r} \frac{\partial}{\partial r} r \frac{\partial}{\partial r} - \frac{(m \pm L)^2}{r^2} + A^2(2 - 3A^2). \quad (8)$$

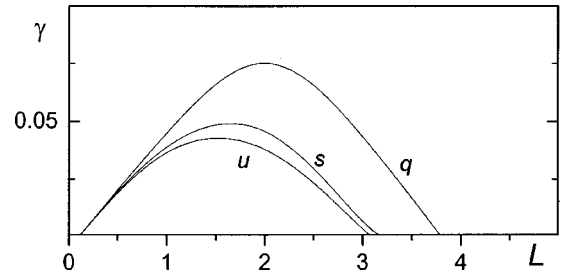


FIG. 4. Growth rate  $\gamma$  as a function of the azimuthal index  $L$  for propagation constant  $\beta=0.10$  (curve  $q$ ),  $\beta=0.13$  (curve  $s$ ), and  $\beta=0.14$  (curve  $u$ ).

Growth rate  $\gamma$  as a function of the azimuthal index  $L$  for different values of propagation constant  $\beta$  and for  $m=1$  is given in Fig. 4. Physically,  $L$  must be an integer to ensure azimuthal periodicity, but it appears in the linearized equation as a real parameter [3].

If the constant  $\beta$  is smaller than the critical value 0.145, LOVS are stable for radial perturbation ( $L=0$ ) but not for azimuthal perturbations. For  $\beta > 0.145$  LOVS become stable (maximal growth rate  $\Gamma=0$ ). OVS is stable in the whole studied range (the corresponding curve coincides with axis  $\beta$  in Fig. 5).

Numerical simulations of Eq. (2) performed using the method of finite differences confirm the stability of an OVS predicted by linear stability analysis. Indeed, the evolution of an OVS stationary state perturbed by Gaussian noise (curve  $i$  in Fig. 2) converges to the stationary state (line  $h$ ) due to the generation of radiation spectrum.

In order to obtain a better insight in nonlinear dynamics of LOVS one can analyze integrals of motion of Eq. (2). For zero boundary conditions it is easy to demonstrate that Eq. (4) conserves the following integrals of motion: the “photon number” (or beam power)

$$N = \int d\mathbf{r}_\perp |E|^2, \quad (9)$$

the Hamiltonian

$$H = \int d\mathbf{r}_\perp (|\nabla_\perp E|^2 - |E|^4/2 + |E|^6/3), \quad (10)$$

and the angular momentum

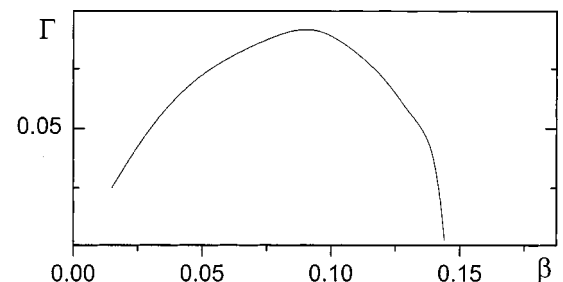


FIG. 5. For  $\beta < 0.145$  LOVS is unstable (maximal growth rate  $\Gamma \neq 0$ ) but it becomes stable for  $\beta > 0.145$ . OVS is stable in the whole examined range.

$$M = \frac{i}{2} \int d\mathbf{r}_\perp \left[ x \left( E^* \frac{\partial E}{\partial y} - \text{c.c.} \right) - y \left( E^* \frac{\partial E}{\partial x} - \text{c.c.} \right) \right]. \quad (11)$$

Any initial field distribution has to conserve these integrals during their evolution. Following Zakharov *et al.* [5], if the Hamiltonian is negative there is no diffraction since the maximum value of the field intensity has a  $z$ -independent lower bound  $|E|_{\max}^2 > 2|H|/N$ . Saturating nonlinearity prevents the wave collapse to develop. As a consequence, the beam is self-trapped. For steady state solution, i.e.,  $E = E_0(x, y) \exp(i\beta z)$  the Hamiltonian is

$$H = -\frac{1}{6} \int d\mathbf{r}_\perp |E_0|^6 < 0. \quad (12)$$

Therefore the LOVS appears to be in the self-trapped regime and consequently neither azimuthal nor radial modulation instability leads to either its diffraction or collapse. However, modulation instability usually leads to the beam breaking in multiple filaments. These filaments have to conserve the total angular momentum  $|M| = |m|N$ . Since the fusion of filaments is not possible due to the topological reasons, they can eventually spiral about each other or fly off tangentially to the initial ring generating bright solitonic structures found for index saturation nonlinearity [3]. Our numerical simulations for  $\beta < 0.145$  give evidence of a quickly developing instability. In agreement with predictions of linear stability analysis ( $\gamma = \Gamma$  for  $L = 2$  in Fig. 4) the beam breaks into two filaments running away tangentially in opposite directions without spiraling (see Fig. 6 for  $\beta = 0.1$ ). Both filaments like spatial solitons remain stable [9].

We hope that our results obtained by linear stability analysis can help in resolving a controversy; in Ref. [10]

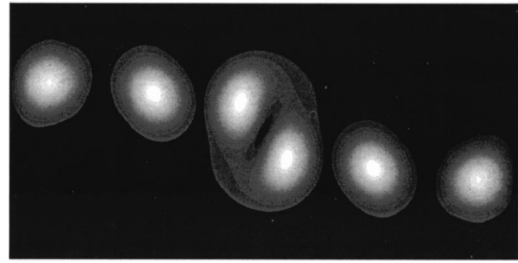


FIG. 6. Break of the beam into two filaments running away tangentially for  $z = 50$ ,  $z = 100$ , and  $z = 160$ .

authors argue that the stability of LOVS for  $\beta > 0.145$  [8] is observed most probably due to an insufficiently long run. We also simulated, for different  $\beta$ , the evolution of an initial stationary state perturbed radially and azimuthally by Gaussian noise. In order to be sure that some very slow instability is not developing we performed numerical simulations until  $z = 6000$ , i.e., for 150 soliton periods  $Z_o = 2\pi/\beta \approx 40$ . Our simulations confirm the result of Ref. [8]. With the increase of  $\beta$  ( $0.145 < \beta < 3/16$ ) curves for LOVS and OVS (respectively,  $p$  and  $o$  in Fig. 3) converge suggesting the similar stability properties.

We established a novel kind of stable OVS in the focusing–defocusing optical and other media. The linear stability analysis and numerical simulations confirm the stability of LOVS in the defocusing region and show its breaking into filaments in a focusing one. We demonstrated the coexistence of LOVS and OVS solutions in such media due to the cubic–quintic nonlinearity switching from the self-focusing to the self-defocusing regime and vice versa. Such a switching may open for different kinds of materials a new domain of potential applications for integrated all-optical signal processing.

- 
- [1] G. A. Swartzlander, Jr. and C. Law, *Phys. Rev. Lett.* **69**, 2503 (1992); Yu. S. Kivshar and B. Luther-Davies, *Phys. Rep.* **298**, 81 (1998).
- [2] J. Atai, Y. Chen, and J. M. Soto-Crespo, *Phys. Rev. A* **49**, R3170 (1994); V. Tikhonenko, J. Christou, and B. Luther-Davies, *J. Opt. Soc. Am. B* **12**, 2046 (1995); *Phys. Rev. Lett.* **76**, 2698 (1996).
- [3] W. J. Firth and D. V. Skryabin, *Phys. Rev. Lett.* **79**, 2450 (1997); D. V. Skryabin and W. J. Firth, *Phys. Rev. E* **58**, 3916 (1998).
- [4] N. R. Heckenberg, R. McDuff, C. P. Smith, and A. G. White, *Opt. Lett.* **17**, 221 (1992); M. W. Beijersbergen, R. P. C. Coerwinkel, M. Kristensen, and J. P. Woerdman, *Opt. Commun.* **112**, 321 (1994).
- [5] V. E. Zakharov, V. V. Sobolev, and V. C. Synakh, *Zh. Eksp. Teor. Fiz.* **60**, 136 (1971) [*Sov. Phys. JETP* **33**, 77 (1971)]; C. Zhou, X. T. He, and S. Chen, *Phys. Rev. A* **46**, 2277 (1992).
- [6] E. C. Jossierand and S. Rica, *Phys. Rev. Lett.* **78**, 1215 (1997).
- [7] B. L. Lawrence, *et al.*, *Phys. Rev. Lett.* **73**, 597 (1994); E. M. Wright, B. L. Lawrence, W. Torruellas, and G. Stegeman, *Opt. Lett. OPLEDP* **20**, 2481 (1995); B. L. Lawrence and G. Stegeman, *ibid.* **23**, 591 (1998).
- [8] M. Quiroga-Teixeiro and H. Michinel, *J. Opt. Soc. Am. B* **14**, 2004 (1997).
- [9] V. Skarka, V. I. Berezhiani, and R. Miklaszewski, *Phys. Rev. E* **56**, 1081 (1997).
- [10] D. Mihalache, *et al.*, *Phys. Rev. E* **61**, 7142 (2000).